



**DEPARTMENT
OF
MECHANICAL ENGINEERING**

**Quarterly Progress Report #5, NAS8-20284
VIBRATION EFFECTS ON HEAT TRANSFER
IN CRYOGENIC SYSTEMS**

July 1, 1967 - September 30, 1967

**ENGINEERING AND
INDUSTRIAL RESEARCH STATION**

FACILITY FORM 802	N68-10178	
	(ACCESSION NUMBER)	(THRU)
	43	1
	(PAGES)	(CODE)
	68-89959	33
	(NASA CR OR TMX OR AD NUMBER)	(CATEGORY)

**MISSISSIPPI STATE UNIVERSITY
STATE COLLEGE, MISSISSIPPI**

Department of Mechanical Engineering
Mississippi State University
State College, Mississippi 39762

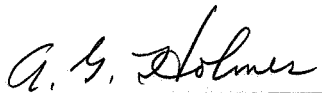
Quarterly Progress Report #5, NAS8-20284
VIBRATION EFFECTS ON HEAT TRANSFER
IN CRYOGENIC SYSTEMS

Period Covered: July 1, 1967 - September 30, 1967

By

C. T. Carley, Associate Professor
C. J. Bell, Associate Professor
T. T. Crow, Associate Professor
R. E. Forbes, Graduate Assistant
G. V. Smith, Graduate Assistant
G. T. Shivers, Graduate Assistant

Approved By:



A. G. Holmes, Head
Mechanical Engineering Department

Quarterly Progress Report #5
Contract Number: NAS8-20284

This report was prepared by Mississippi State University under Contract NAS8-20284, Vibration Effects on Heat Transfer in Cryogenic Systems, for the George C. Marshall Space Flight Center of the National Aeronautics and Space Administration. The work was administered under the technical direction of the Propulsion and Vehicle Engineering Laboratory of the George C. Marshall Space Flight Center with Mr. Bill Dickson acting as project manager.

TABLE OF CONTENTS

	Page
List of Figures	iv
Nomenclature	vi
Introduction	1
Progress	2
WATER TEST SYSTEM.	2
Heat Transfer Results.	2
Temperature Profiles	5
Flow Visualization.	8
LIQUID NITROGEN TEST SYSTEM	12
Progress Expected During the Next Report Period	15
Appendix	34

LIST OF FIGURES

Figures	Page
1. Effect of Vibration on Heat Transfer Enclosure Velocity = 1.70 in./sec.	16
2. Effect of Vibration on Heat Transfer Enclosure Velocity = 1.70 in./sec.	17
3. Effect of Vibration on Heat Transfer Enclosure Velocity = 1.70 in./sec.	18
4. Effect of Vibration on Heat Transfer Enclosure Velocity = 1.70 in./sec.	19
5. Effect of Vibration on Heat Transfer Enclosure Velocity = 1.70 in./sec.	20
6. Effect of Vibration on Heat Transfer.	21
7. Dimensionless Temperature Profiles: No Vibration.	22
8. Dimensionless Temperature Profiles: Enclosure Vibration 4000 cps 25 g.	23
9. Dimensionless Temperature Profiles: Enclosure Vibration 1280 cps 25 g.	24
10. Dimensionless Temperature Profiles: Enclosure Vibration 320 cps 9 g.	25
11. Dimensionless Temperature Profiles: Enclosure Vibration 80 cps 12 g.	26
12. Flow Patterns - Streak Method (see appendix)	27
13. Flow Patterns - View Interruption Method (see appendix)	28
14. Flow Patterns - Entire Cell (see appendix)	29
15. Flow Visualization View Interruption Wheel.	30
16. Acceleration Levels at Various Points on the Enclosure Relative to Table Acceleration (g_t).	31

LIST OF FIGURES (continued)

Figures	Page
17. Liquid Nitrogen Test System.	32
18. Bellows Mounting Detail	33

NOMENCLATURE

T'_h	-	Hot plate surface temperature
T'_c	-	Cold plate surface temperature
T'	-	Fluid temperature
x'	-	Horizontal coordinate measured from hot plate
y'	-	Vertical coordinate measured from bottom of enclosure
W'	-	Enclosure width
H'	-	Enclosure height
Ra	-	$= (T'_h - T'_c) \bar{\beta}' W'^3 g'_0 / \alpha' \nu'$ Rayleigh Number
Nu	-	$= h' W' / k'$ Nusselt Number

INTRODUCTION

The research efforts during this report period were directed primarily at two of the objectives of this project. The production of a complete set of data on the first aspect ratio of the water test cell constituted the first effort. The second effort consisted of the completion of the design for the liquid nitrogen test cell and the beginning of its construction.

Since no information is available in the technical literature concerning the effect of vibration on natural convective heat transfer in enclosures, it was felt imperative to obtain high quality data. A complete set of such data over a wide range of the variables involved is necessary before further progress can be made toward improving the analytical solution already in hand. This report describes the efforts toward achieving a complete set of data and the decisions involved concerning the type of data to be recorded.

The design of a liquid nitrogen test system, which was begun at the start of this report period, has been completed. Subsequent to completion of the design, construction of the major components was begun and several of these components have been constructed.

Information concerning the two efforts described above consists of the presentation of a part of the data which was recorded from the water test system and a description of the major design aspects of the liquid nitrogen test system.

PROGRESS

WATER TEST SYSTEM

The accumulation of data using water as the test fluid was started at the beginning of this report period. Subsequent to solving some routine apparatus and instrumentation problems, a total of 42 data points was recorded. These data are considered to be the primary information taken from the system since they show directly the effect of mechanical vibration on convective heat transfer in an enclosure. Also recorded during this report period were large amounts of data from the traversing thermocouples and from the flow visualization apparatus. These three areas will be discussed separately.

Heat Transfer Results

With the test cell as constructed and integrated into the electrodynamic vibration facility, the following ranges of variables were available.

Temperature Difference Across the Cell 0° to 110° F.

Vibration Frequency 0 to 4000 cps

Acceleration Level 0 to 110 g

A qualitative analysis was performed in order to select a procedure for accumulating data. It was first necessary to decide whether to establish a thermal field and then impose a vibration field upon it or to establish these fields in the reverse order. In the light of the expected practical applications for the information to be produced,

it was decided to first establish a thermal field in the test system and then to impose different vibrational stresses on the cell. Following this decision, it was necessary to establish a procedure for recording the data.

Out of an almost infinite number of combinations, the following was selected. A chosen temperature difference was established across the test cell. This required balancing of electrical heaters until isothermal conditions were established on the hot plate. This was done under a no vibration condition. At this point temperatures and power input to the heaters were recorded in order to determine the cell heat transfer characteristics.

The shaker was then energized and brought to a preselected frequency. At this frequency the amplitude was adjusted to achieve a maximum acceleration level within the capability of the apparatus. The system parameters were then monitored until equilibrium had been achieved. No effort was made to readjust the temperature of the hot plate to its initial value but the variation of temperature over the height of the hot plate and cold plate was recorded. It was felt that this procedure would produce more useful results for immediate application.

The above procedure was followed for temperature differences of 20, 40, 60, 80 and 100 degrees Fahrenheit and for vibrational frequencies of 20, 80, 320, 1280 and 4000 cycles per second. Subsequent to the recording of the above data, another series of tests was run at constant enclosure velocities.

A study of the technical literature available in this area indicates that average surface velocity provides the most satisfactory variable

with which to correlate the heat transfer data in a vibrating system. On the basis of this, an enclosure velocity was selected which could be reached over the entire range of frequencies available. The enclosure velocity is defined as the product of the amplitude and frequency of vibration. The velocity selected was 1.70 inches per second.

This second series of tests was run with the same procedure as the first except that at each frequency the amplitude was selected to produce an enclosure velocity of 1.70 inches per second rather than a maximum acceleration.

A digital computer program was written to convert the raw data into the dimensionless parameters Nusselt number and Rayleigh number.

Since study and analysis of the data recorded is incomplete, only a portion of the data will be presented here. Figures 1 through 5 show the results of the second series of tests taken at constant enclosure velocity. This data is presented in the form of Nusselt number versus Rayleigh number at constant enclosure velocity with the frequency and acceleration levels required to produce this velocity indicated on each curve. The general trend of the data shown in these figures is to indicate, as might be expected, that the vibration increases the heat flux. A maximum increase of approximately 30% was found at a frequency of 1280 cycles per second and 36 g's.

The first set of data accumulated under the procedure described above is presented here in Figure 6. This information will be discussed in the following Quarterly Report after sufficient analysis has been performed.

Temperature Profiles

In an attempt to determine the detailed characteristics of the thermal field within the enclosure, temperature profiles were recorded as described below. The cell was instrumented with seven small, butt-welded thermocouples suspended across its width at evenly spaced vertical intervals. These thermocouples could be moved longitudinally thus placing the thermocouple junction at any desired horizontal position. These thermocouples were located in a vertical plane at the midpoint of the depth of the cell in order to avoid end effects.

The procedure for data collection with these thermocouples was as follows. The width of the cell was arbitrarily broken up into tenths. Each thermocouple junction was positioned by visual alignment with two vertical reference lines on either end of the cell. Temperatures were recorded at each of the 1/10 increments across the cell and, in addition, at the 0.05 positions near the walls. Thus, a total of eleven temperatures were recorded by each thermocouple across the width of the cell. These eleven temperatures combined with the readout of the thermocouples embedded in the surfaces of the hot and the cold plates yielded temperature profiles across the width of the cell which are presented in Figures 7 through 11. At each condition of temperature difference and vibrational stress, a temperature profile was recorded. This involved locating each of the seven thermocouple junctions sequentially at each of the eleven transfer positions. This yielded 22 temperature recordings at each of 42 cell test conditions for a total of 924 recorded temperatures.

The temperature profiles are presented in dimensionless form in Figures 7 through 11 for one of the cell temperature differences recorded,

that of 20° F. Similar temperature profiles have been drawn for the other four ΔT 's but are not presented here for reasons of economy.

In order to make temperature dimensionless, the same scheme was selected that had been used in the analytical approach. The temperature traverses shown were routinely checked for reproducibility and excellent results were indicated in all cases. One interesting phenomenon developed which should be noted. When the thermocouple junctions were placed at the stations in closest proximity to the walls, periodic temperature fluctuations were noticed. These fluctuations began at a position about 1/3 of the height from the bottom of the cell and increased in intensity toward the top of the cell. These fluctuations could be correlated visually with a "waviness" of the boundary layer along the hot and cold plates. These fluctuations are apparently associated with the traveling waves which precede transition from laminar to turbulent boundary layer characteristics. An attempt was made to instrument these thermocouples with strip chart recorders in order to determine frequency distributions. It was soon discovered, however, that extensive shielding would be necessary in order to satisfactorily record these fluctuations and the effort was dropped as it was considered to be of peripheral interest.

The following section will describe the apparatus used and results obtained from the flow visualization study. As a part of this study it was noticed that there were apparent three-dimensional effects in the flow in the neighborhood of the traversing thermocouples. There appeared to be a variety of these three-dimensional flow patterns and no consistency could be detected. As a result of this observation, it was suspected

that the traversing thermocouples were vibrating under the vibrational stress applied to the cell thus producing a stirring action. As a result of this suspicion, the traversing thermocouples were removed and two reproducibility runs were attempted. The following table indicates the results.

	Traversing Thermocouples Installed	Traversing Thermocouples Removed
No Vibration:	Nu = 14.16 Ra = 3.7×10^7	Nu = 14.61 Ra = 3.61×10^7
4000 cps: 110 g	Nu = 14.72 Ra = 3.46×10^7	Nu = 15.2 Ra = 3.4×10^7

Table 1. Effect of Traversing Thermocouples on Cell Heat Flux.

At the vibratory conditions shown, the effect of the traversing thermocouple appears to be negligible. It is anticipated, however, that this effect could be quite significant at the natural mode of vibration of the suspended thermocouple. Further data will be taken along these lines in an attempt to determine the effect of the traversing thermocouples over the entire range of variables.

The dimensionless temperature profiles presented in Figures 7 through 11 show some interesting characteristics. These characteristics must be interpreted in the light of the flow patterns which develop within the

cell. Further discussion of this point will be provided in the next Quarterly Report after all the data have been analyzed.

Flow Visualization

As described in previous reports, the method selected for flow visualization makes use of neutrally bouyant particles. These small hollow glass spheres follow stream lines with great integrity and, as well, provide excellent reflection of light for photographic recording of their paths.

An extensive series of preliminary tests was conducted in an effort to determine the characteristics of these small particles. As received from the manufacturer (Emerson and Cuming, Inc.) these eccospheres range in size from 0.0017 to 0.0059 inches. A typical sample when placed in motionless water exhibits the characteristic of settling of some of the nonuniform particles and ascension of the larger particles. It was found that the smallest particle sizes remained neutrally bouyant. The particles were then graded by screening into five categories: 0.0017 to 0.0021, 0.0021 to 0.0029, 0.0029 to 0.0041, 0.0041 to 0.0059 and greater than 0.0059. Similar tests on these categories indicated that the previous conclusion was valid, that is, that the smallest particles were the most neutrally bouyant. A microscopic investigation of the size distribution and quality of these eccospheres was carried out.

Motion of these particles was recorded in the following manner. A collimated light beam with a width of approximately 1/4 of an inch was projected vertically through the test cell from above. When viewed from a horizontal position, motion of these particles was visible in this plane of light. Records of particle motion were made with the use of a 4" x 5"

Speed Graphic camera.

Another series of preliminary experiments was conducted in the cell to determine the optimum density of particles. It was found that there is not a single density which will serve for all conditions of illumination and vibration. In most cases, however, it was found better to err on the side of too few particles rather than too many. As a general rule, density of approximately 1/100 of a gram per gallon was found to be sufficient.

The flow visualization techniques were divided into two efforts. The first was to obtain uninterrupted photographs of the particles which produced flow paths and yielded general information concerning the patterns formed in the cell. The second effort attempted to use a repetitively interrupted view technique in order to produce traces on the photographic plate which appeared as dashed or dotted lines. Knowledge of the frequency of interruption and measurement of the distances covered by the particles in terms of the number of dashes would then yield quantitative information on velocities. Several modifications of this technique were attempted. It was found that due to the complexity of the flow patterns, information was needed on the direction of travel of each particle. This information was made visible on photographic plates by using a slotted wheel rotating in front of the camera lens. To make the particle images on the photographic plate appear as dashes, slots of uniform cross section were used. An attempt was made to use slots of variable cross section which would produce dashes on the photographic plates which were larger on one end than on the other. In this manner each dash would appear as a vector and particle directions, as well as speeds, could be determined by interpretation of the photographic plates. A sketch of the view interruption

wheel is shown in Figure 15. A difficulty was encountered, however, in that the portion of the slot with a small area produced a paralax problem. An alternate method using a translucent material over a portion of each slot was tested. This technique improved results significantly.

A total of more than 125 photographic plates were exposed during this report period. Three samples of these plates are attached as Figures 12, 13 and 14. Figure 12 shows the upper half of the cell using the streak photograph technique. Figure 13 is an example of the dashed images produced when using a rotating slotted wheel for light interruption. Figure 14 is a view of the entire cell utilizing the streak technique. A descriptive discussion of these figures is given in Appendix I.

It has been found extremely difficult to interpret the results produced by the flow visualization techniques described above. The reasons for this difficulty are manifold and only the primary reasons will be discussed here.

The technique of image production with uninterrupted light producing streak photographs is satisfactory for a gross qualitative interpretation of flow patterns. In order to extract quantitative information on direction and magnitude of the flow at any point within the cell, it appears necessary to use the interruption technique described above. It has been found difficult, if not impossible, to extract consistent data from these photographic plates. The primary reason for this is the apparent three-dimensional flow which occurs over portions of the cell. That is to say, a single particle will not always remain in the plane of light for a period of time sufficient to make quantitative measurements. There appear to be three reasons for this three-dimensionality in the flow field.

The first of these are the large transverse vibrations induced in the cell. These transverse vibrations have been discussed in previous reports and have been recently measured for the cell under study. This information is presented in Figure 16 which shows the ratio of the acceleration level at a particular point on the cell to the acceleration level of the shaker table. It is obvious from this figure that accelerations of sufficient magnitude exist in transverse directions to produce three-dimensional flows and other flow disturbances locally throughout the cell.

The second factor producing three-dimensional flow patterns is the existence of bubble coalescence areas within the cell. Extreme care has been used in an attempt to avoid formation of bubble coalescence areas. These include the use of distilled and degased water and the use of great care to insure complete filling of the cell. It has been found impossible, however, to completely eliminate these areas of bubble coalescence and they appear to have a significant effect on the flow field as well as the thermal field.

The third reason for three-dimensional flow within the cell is the apparent stirring motion produced by the traversing thermocouples as discussed previously. Due to this effect, and the limited value of the temperature profiles, it has been decided to eliminate their use in subsequent runs except in those cases where specifically justified.

One effect of the bubble coalescence phenomenon, which should be mentioned at this point, is to destroy the isothermal condition on the hot plate. The hot plate is adjusted to be isothermal under a nonvibratory state. After the onset of vibratory motion, and in the absence of bubble coalescence areas, the isothermality of the plate never changes more than

2° F. from top to bottom. However, it has been found that when intense areas of bubble coalescence exist that a variation of the temperature of the hot plate of as much as 10° will occur from top to bottom.

In view of the limited success of the photographic technique involving interrupted light beams, it has been decided to attempt flow visualization with neutrally bouyant particles through the use of motion picture photography. The versatility of this method of flow visualization is attractive. It is anticipated that both qualitative and quantitative information can be produced from a single exposure.

LIQUID NITROGEN TEST SYSTEM

Construction of the LN₂ experimental system has begun, with design of auxiliary equipment being finalized as construction proceeds. Construction materials have been selected which are compatible with a liquid nitrogen environment. In cases where design information was lacking, several materials were tested by repeated immersing of the material in LN₂. All construction materials have been selected and are either on hand or have been ordered.

A drawing of the test unit is shown in Figure 17. Construction of the outer cylindrical tank has been completed except for the location of the LN₂ fill lines and the lines to carry electrical and thermocouple leads. The tank was constructed from 6061 aluminum to facilitate rolling and welding. The tank is supported by a channel-iron framework which is bolted to the shaker frame. This method of mounting insures that there will be no relative motion between the tank and the shaker yoke. The tank is

attached to the channel framework using four stainless steel rods in order to minimize conduction losses through the tank support. The tank top and side walls will be insulated with a 5 inch layer of CPR 314-2 foam-in-place urethane foam. The tank bottom will have a 2 inch layer of foam insulation.

Eight stainless steel rods transmit the motion from the shaker table to the aluminum base plate inside the tank. The tank is sealed by stainless steel bellows attached to the tank and the base plate as shown in Figure 18. The heat transfer cell will be bolted to the base plate using stainless steel bolts. Silicon O-rings will be used to seal the bellows assembly at all points where leaks might occur.

The pressure in the LN_2 tank will be maintained at approximately 2 psia by a 105 cubic feet per minute mechanical vacuum pump which has been located in the vicinity of the vibrations laboratory.

The heat transfer cell will be similar to the water-filled test cell which is presently being tested, but it will be smaller. Overall test cell dimensions are 13" high, 10" wide and 6" deep; the electrically heated plate being 10" high and 7.1" wide. The hot plate will be guarded by electric heaters with a phenolic spacer plate located between the guard heaters and the hot plate. The cold plate will be made of aluminum and will be cooled by contact with the LN_2 boiling in the cylindrical tank at 2 psia. Copper-constantan thermocouples will be used to measure hot and cold plate temperatures as well as the temperatures on both sides of the phenolic guard plate. The test cell has been designed so that electrical controls and thermocouple readout equipment presently being used in the water-filled test cell may be used on the LN_2 cell.

Aspect ratios for the LN_2 cell will be identical to those used on the water-filled cell (aspect ratios: 9.3, 15.8 and 31.0).

It is expected that construction will be completed and preliminary testing will be underway at the end of the next quarterly reporting period.

PROGRESS EXPECTED DURING
THE NEXT REPORT PERIOD

The progress expected during the next report period will be in three areas of activity.

The first of these areas will be a continuation of the testing of the water cell with a new aspect ratio. Associated with this will be an analysis of the data presently available as well as that produced from succeeding tests. Flow visualization utilizing motion picture photography will also be attempted during this period.

It is expected that the construction of the liquid nitrogen test system will be completed during the next report period. Instrumentation of this system will also be begun.

A renewal of the analytical portion of this project will constitute the third area of activity in which progress is expected during the next report period. The previous analytical analysis will be viewed in the light of the data now on hand, especially the assumption of bulk liquid motion, and an attempt to improve this analysis will be made.

△ 4000 cps 110 g

⊙ No Vibration

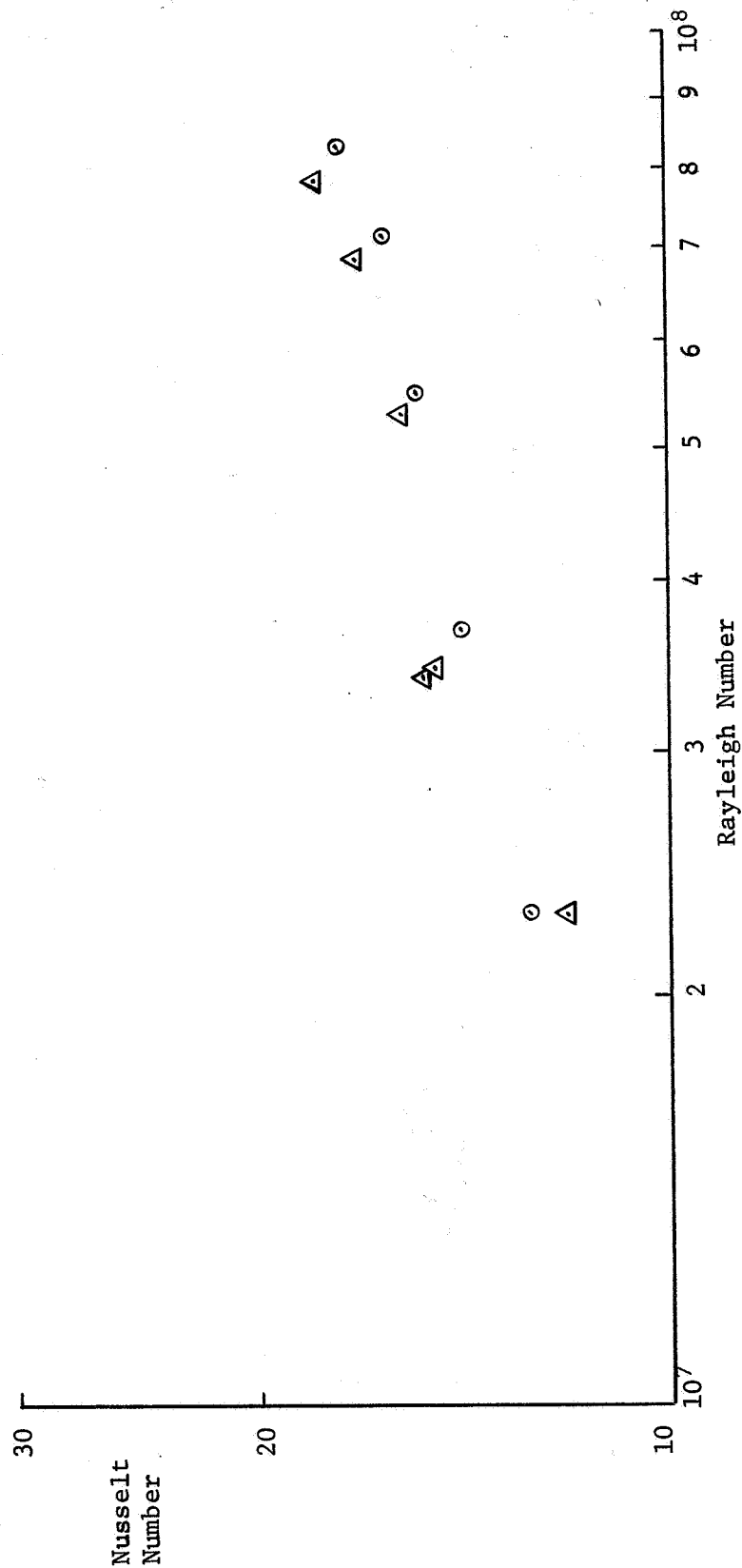


Figure 1. Effect of Vibration on Heat Transfer.
Enclosure Velocity = 1.70 in./sec.

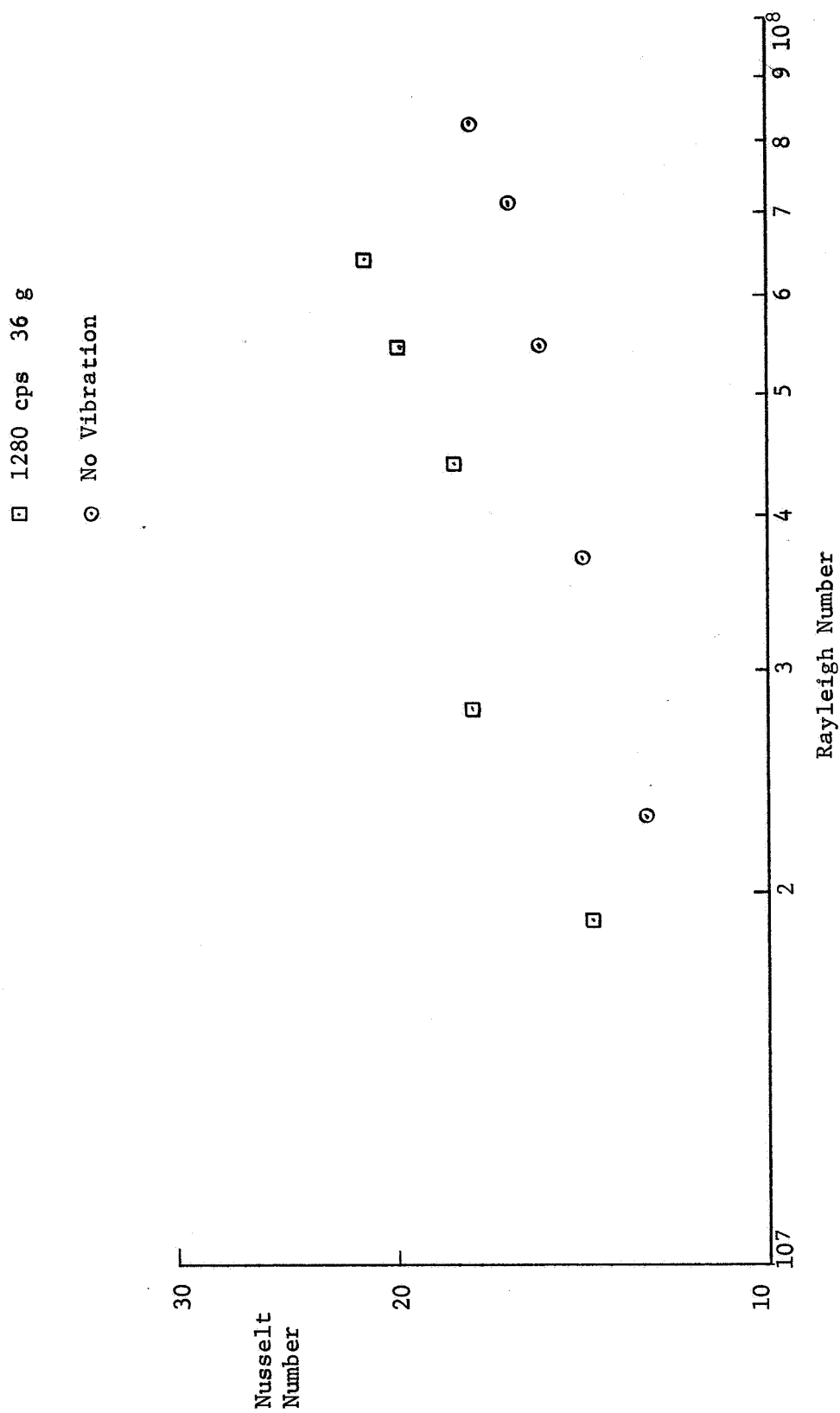


Figure 2. Effect of Vibration on Heat Transfer.
Enclosure Velocity = 1.70 in./sec.

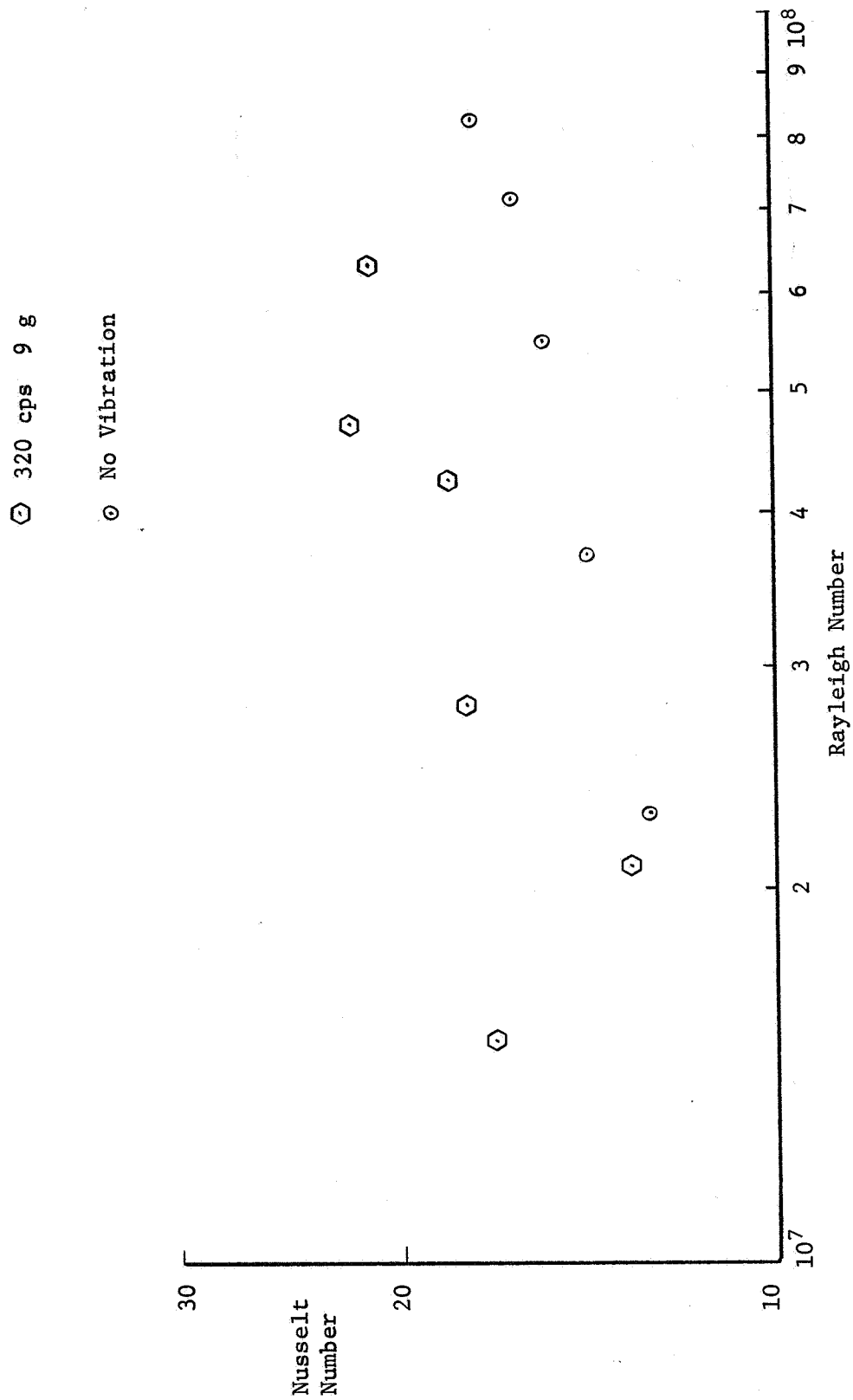


Figure 3. Effect of Vibration on Heat Transfer.
Enclosure Velocity = 1.70 in./sec.

▲ 80 cps 2.2 g
 ○ No Vibration

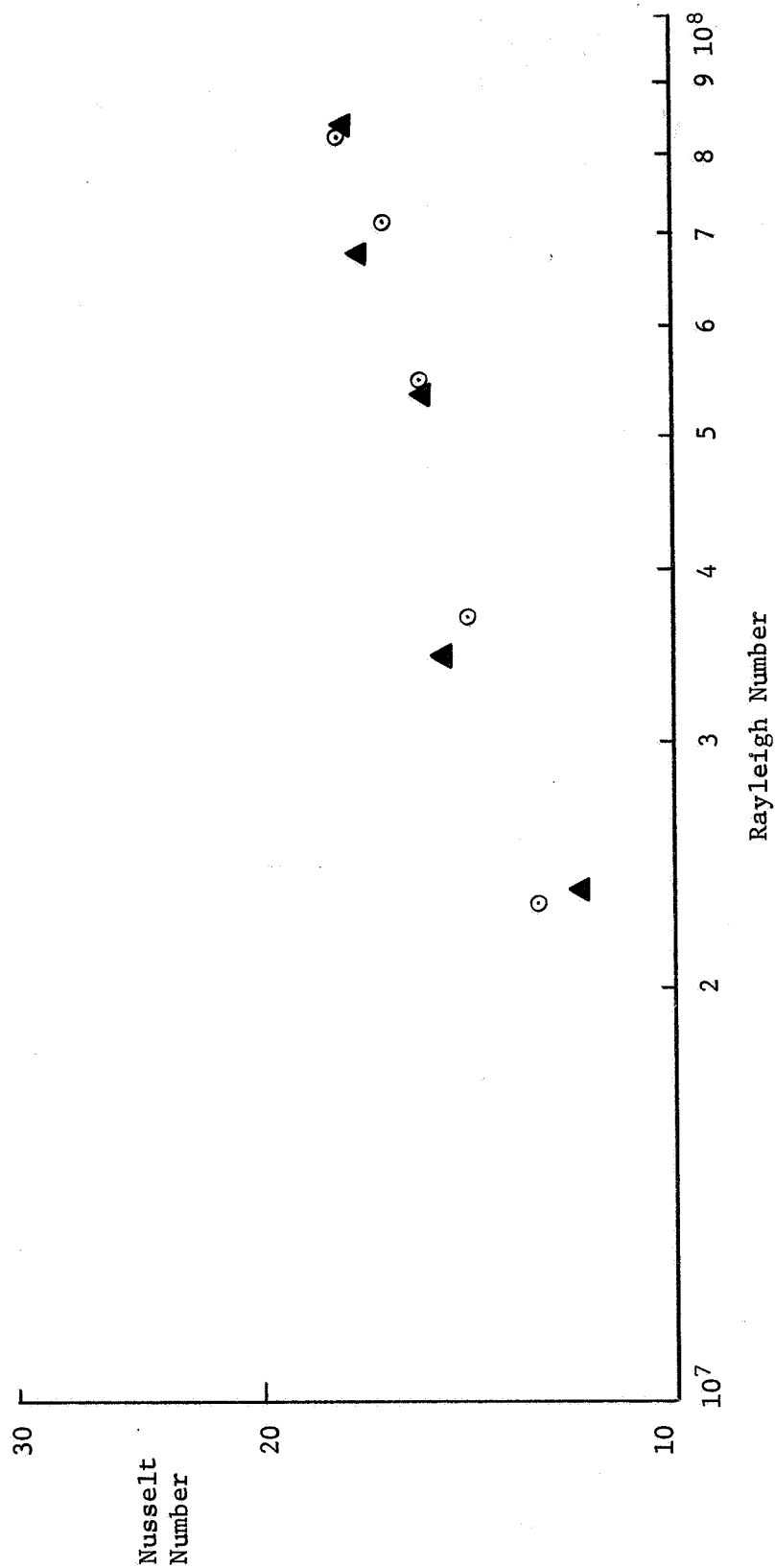


Figure 4. Effect of Vibration on Heat Transfer.
 Enclosure Velocity = 1.70 in./sec.

■ 20 cps .55 g

○ No Vibration

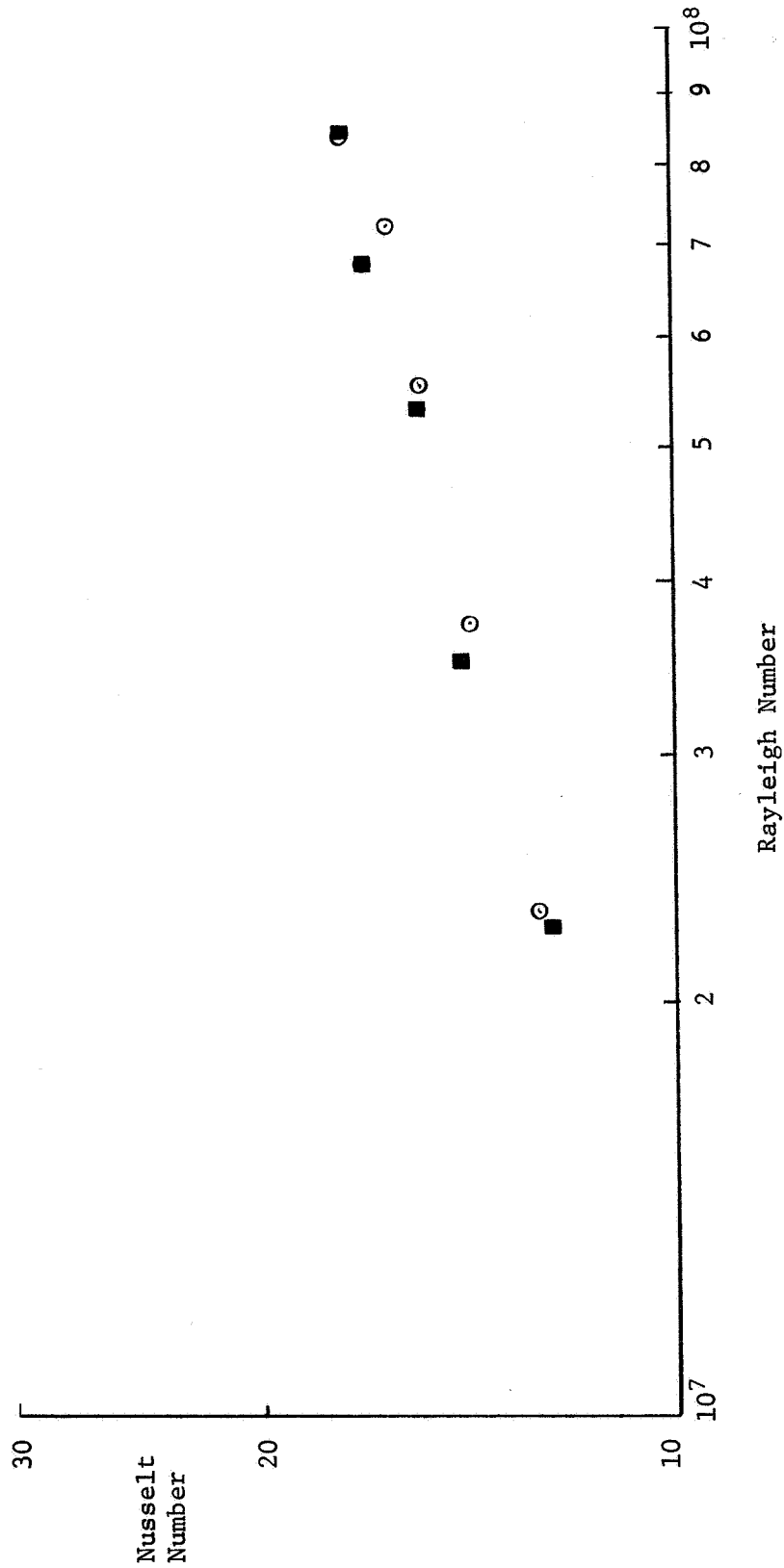


Figure 5. Effect of Vibration on Heat Transfer.
Enclosure Velocity = 1.70 in./sec.

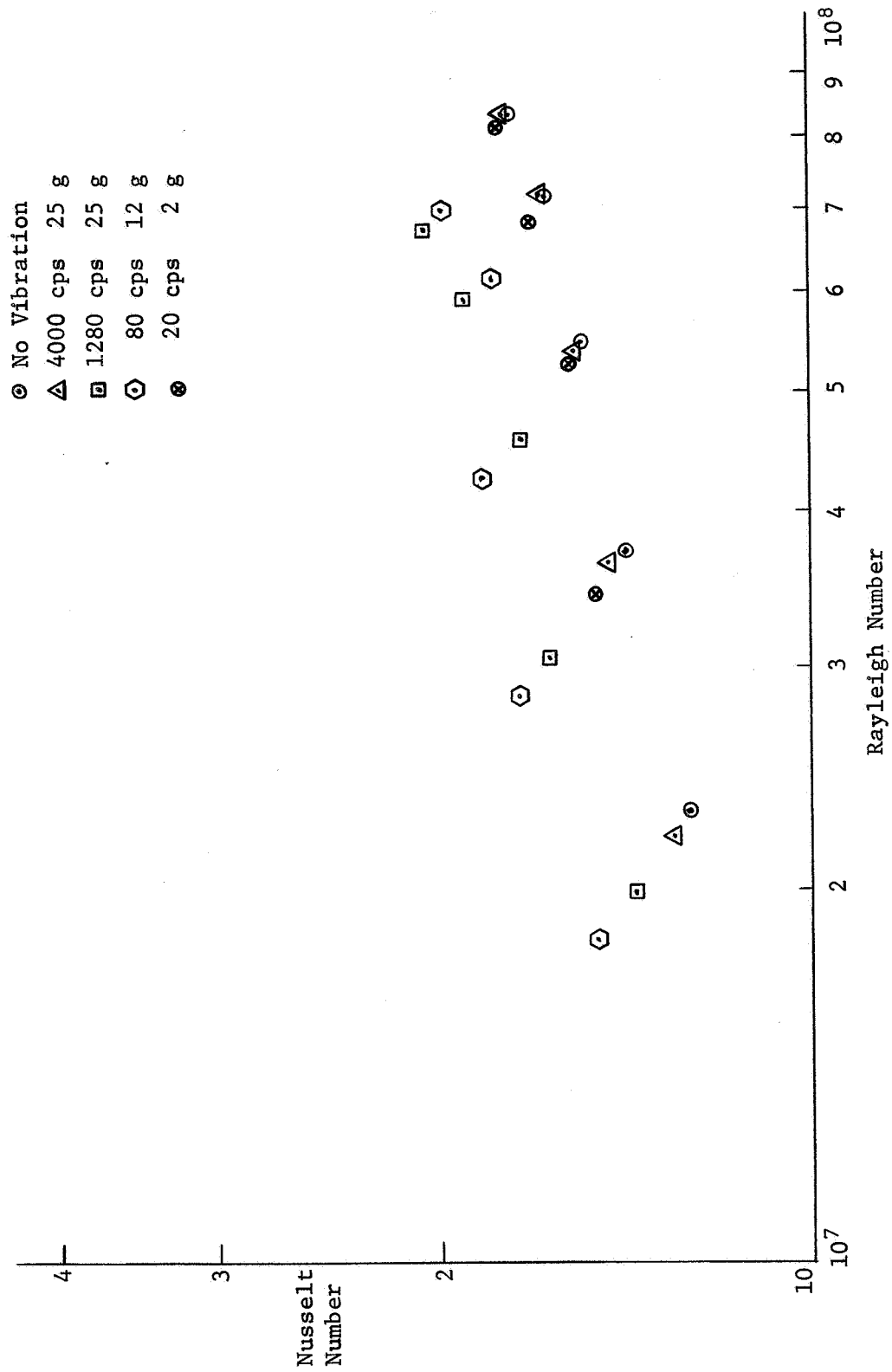


Figure 6. Effect of Vibration on Heat Transfer

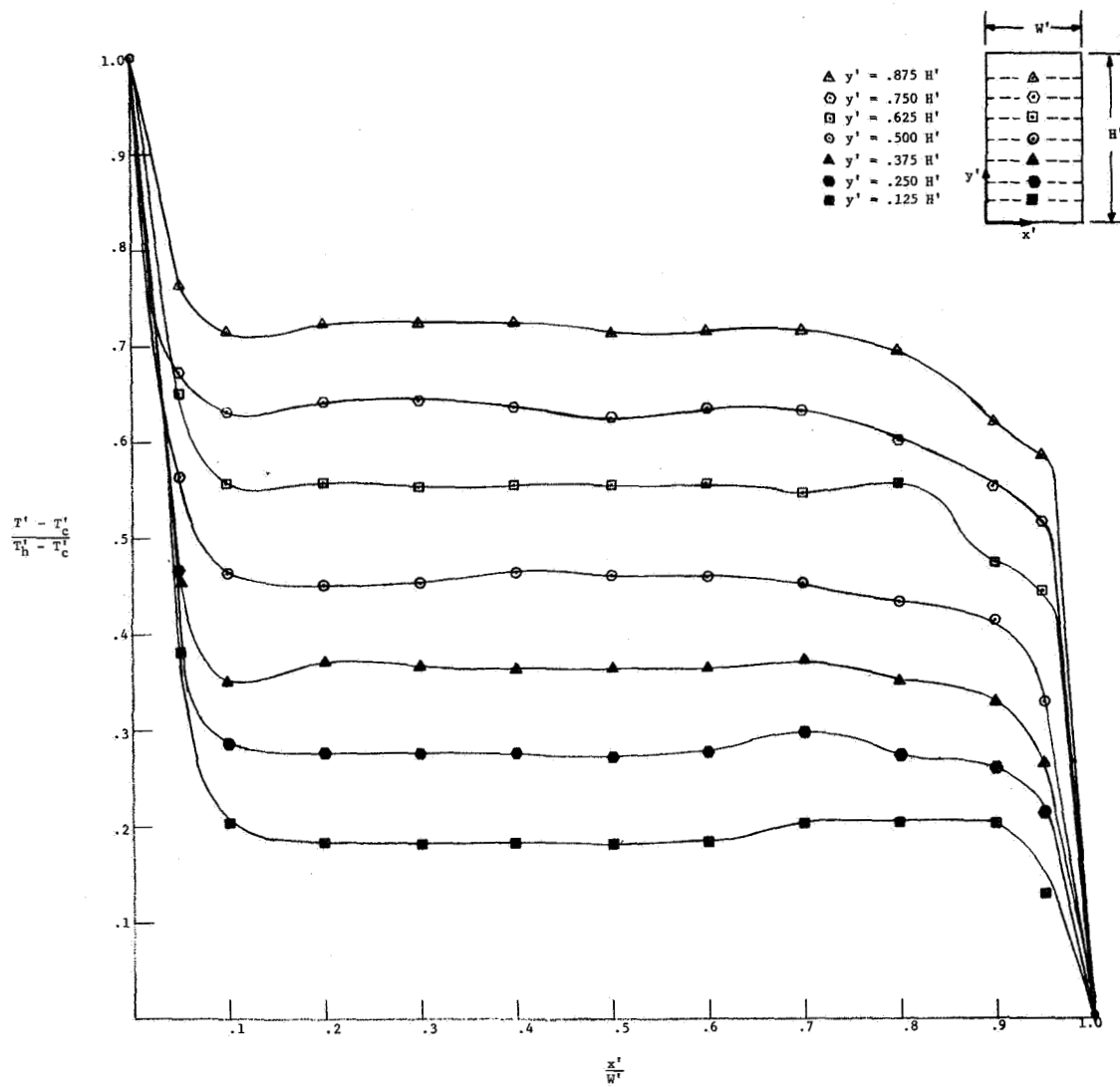


Figure 7. Dimensionless Temperature Profiles: No Vibration

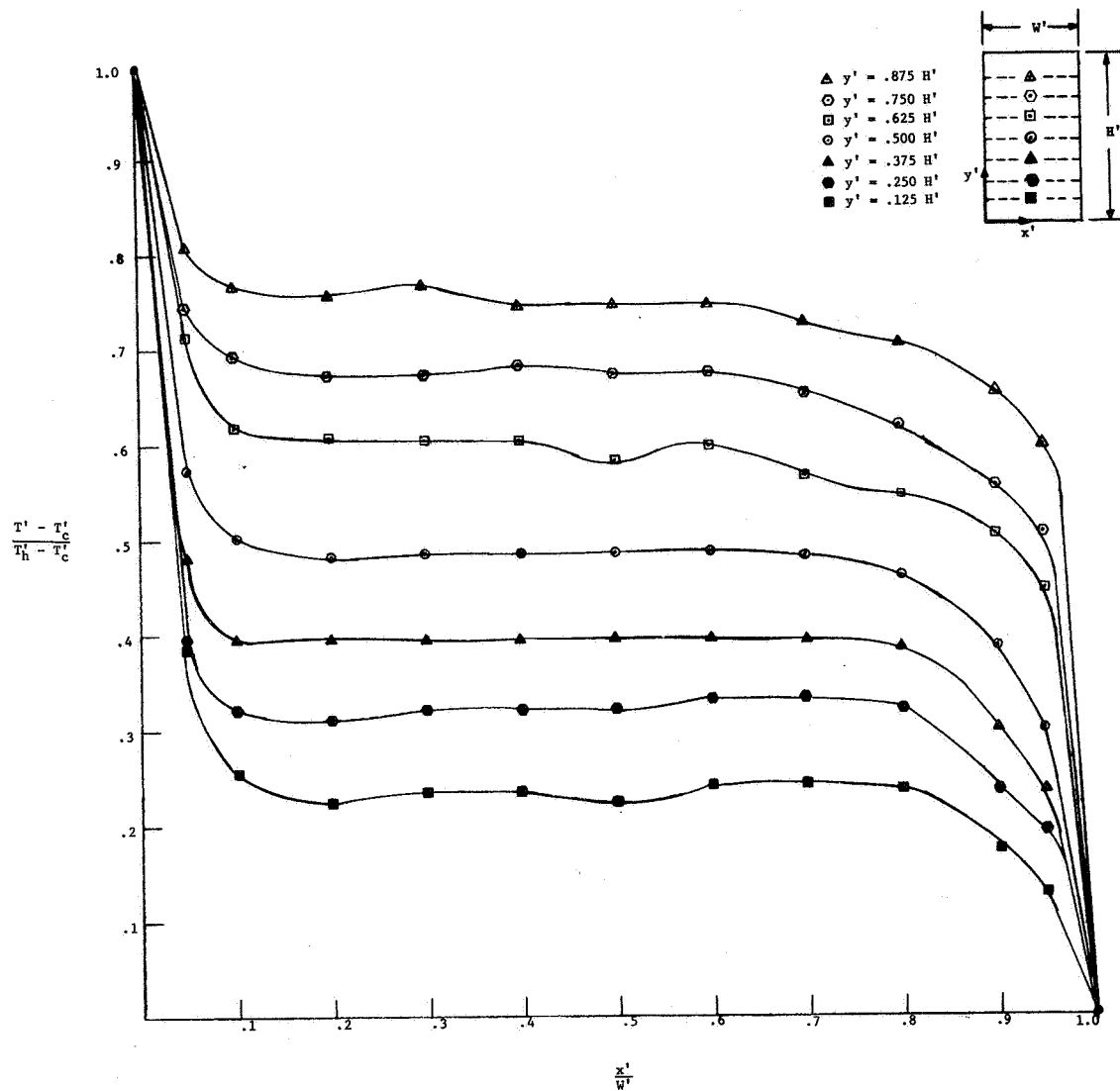


Figure 8. Dimensionless Temperature Profiles:
Enclosure Vibration 4000 cps 25 g

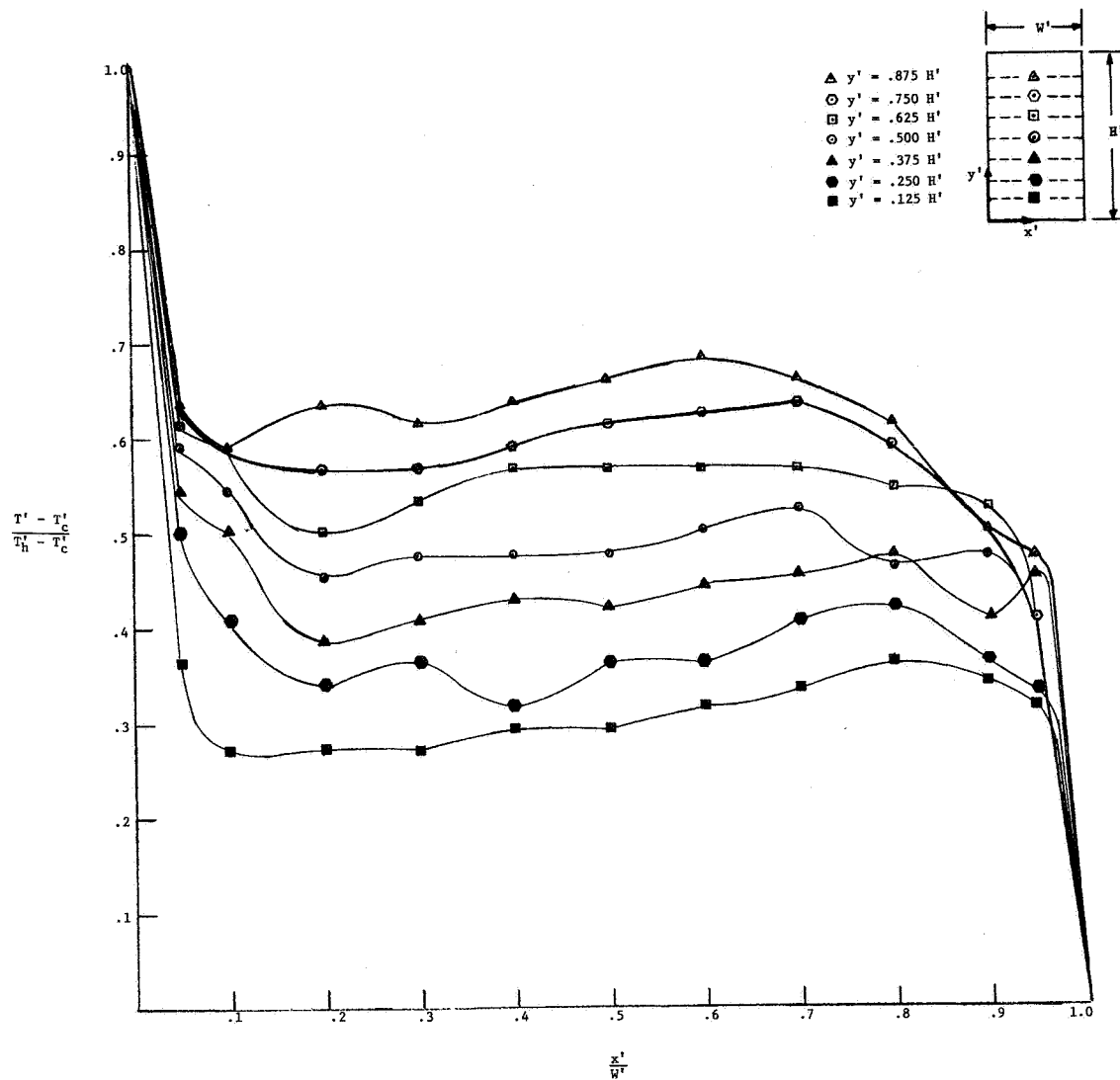


Figure 9. Dimensionless Temperature Profiles:
Enclosure Vibration 1280 cps 25 g

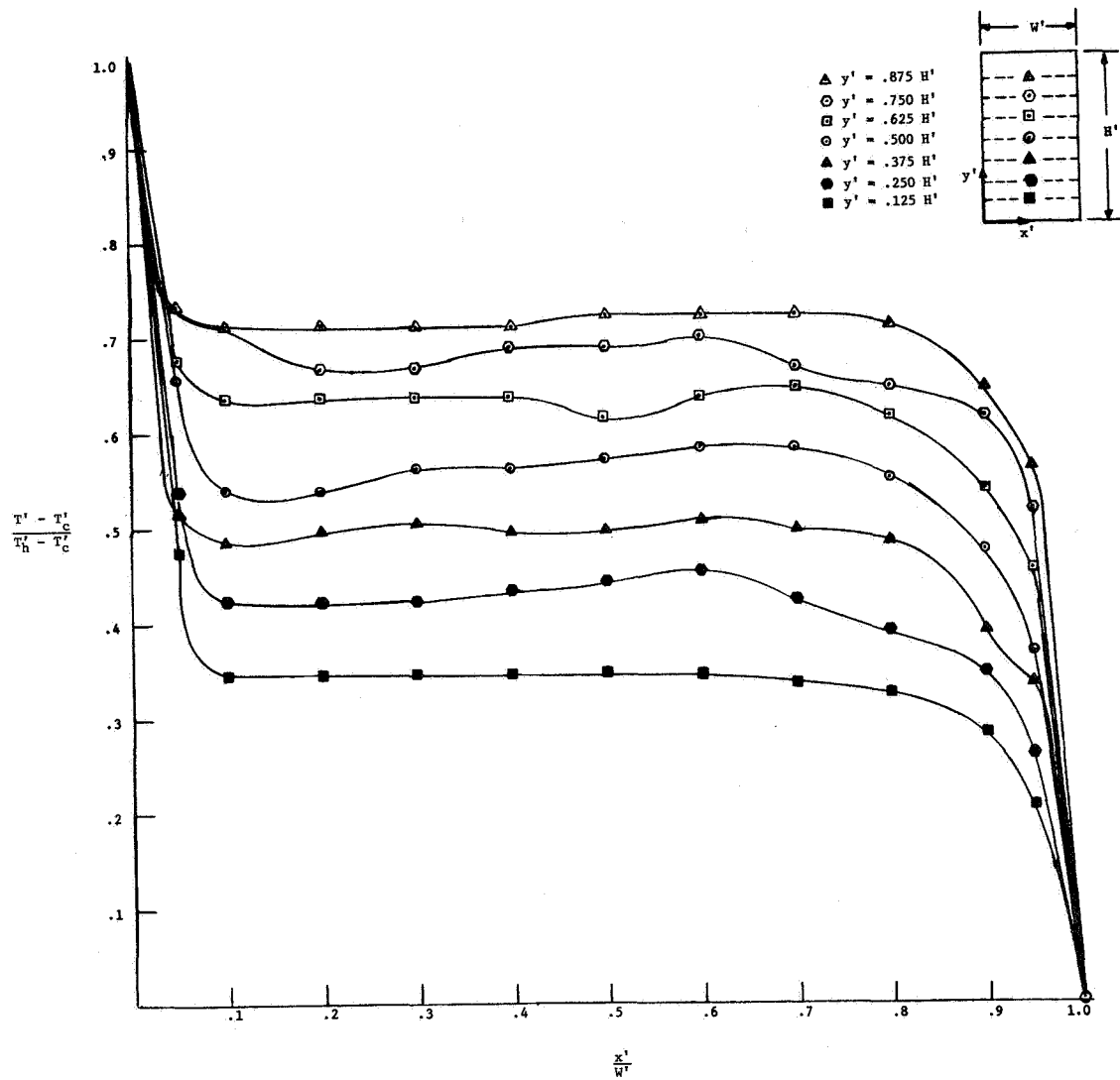


Figure 10. Dimensionless Temperature Profiles:
Enclosure Vibration 320 cps 9 g

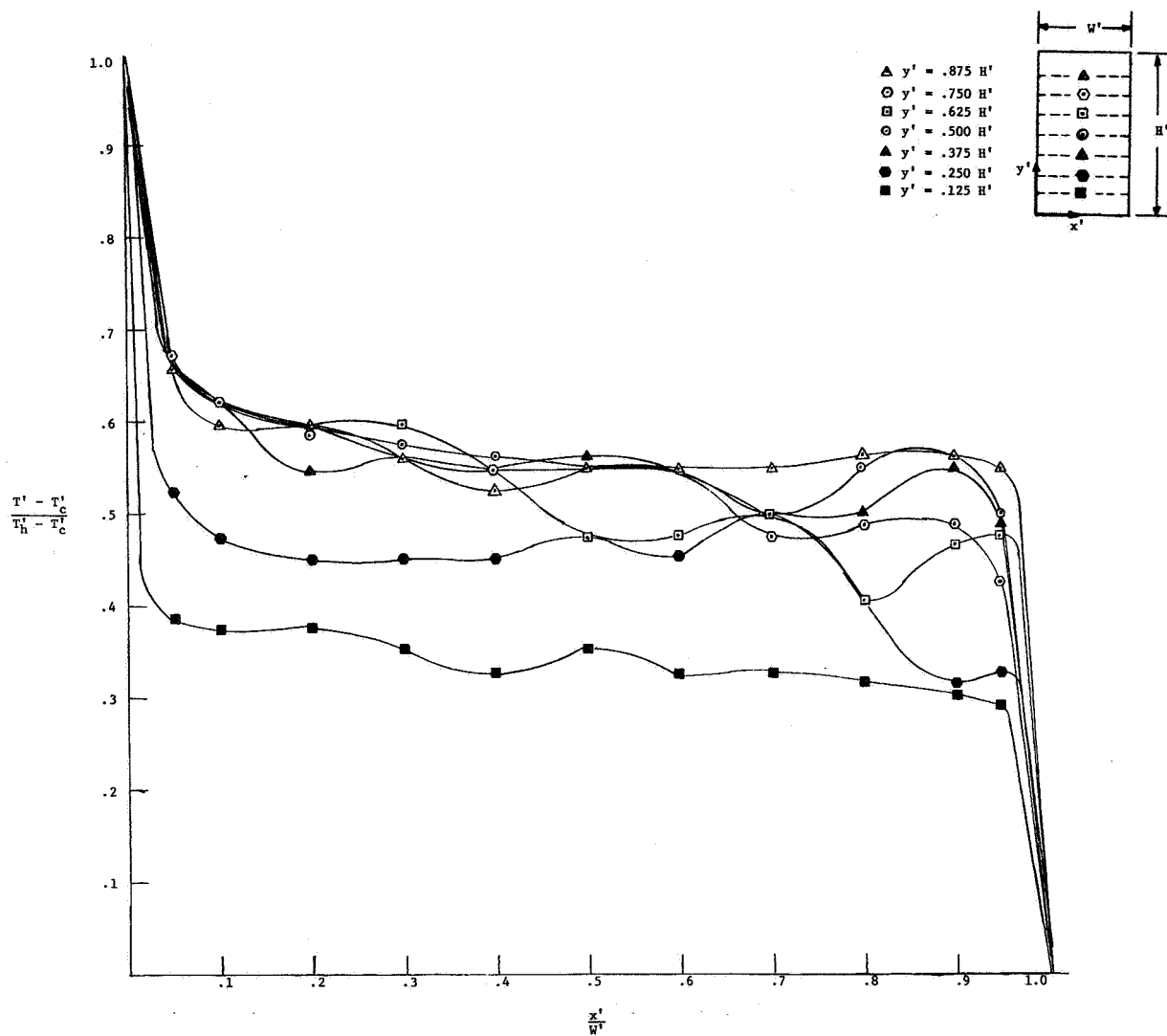


Figure 11. Dimensionless Temperature Profiles:
Enclosure Vibration 80 cps 12 g

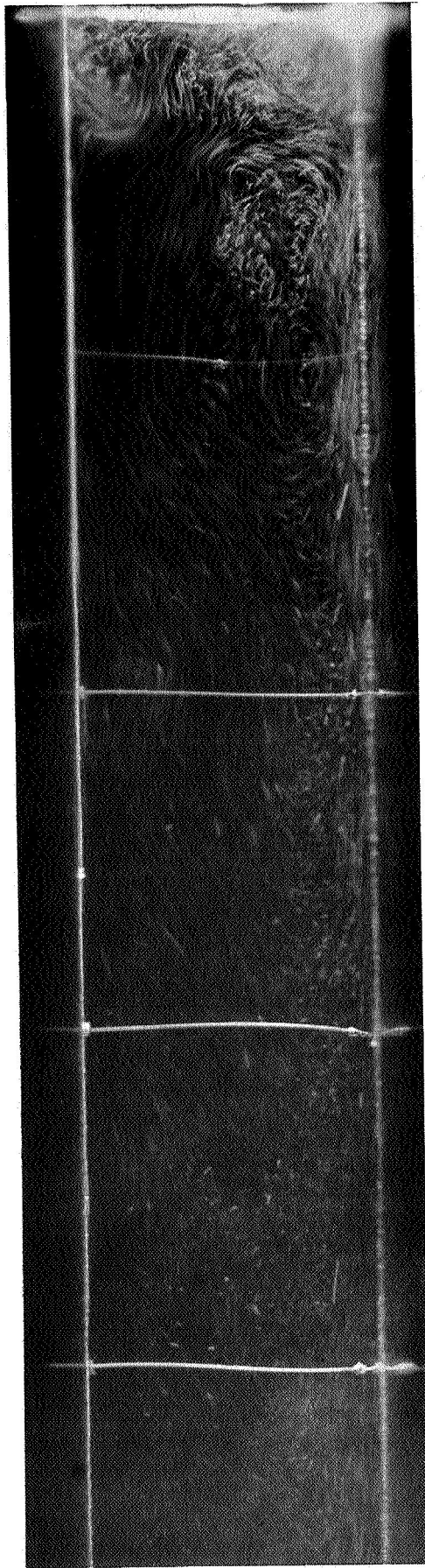


Figure 12. Flow Patterns - Streak Method
(see Appendix)

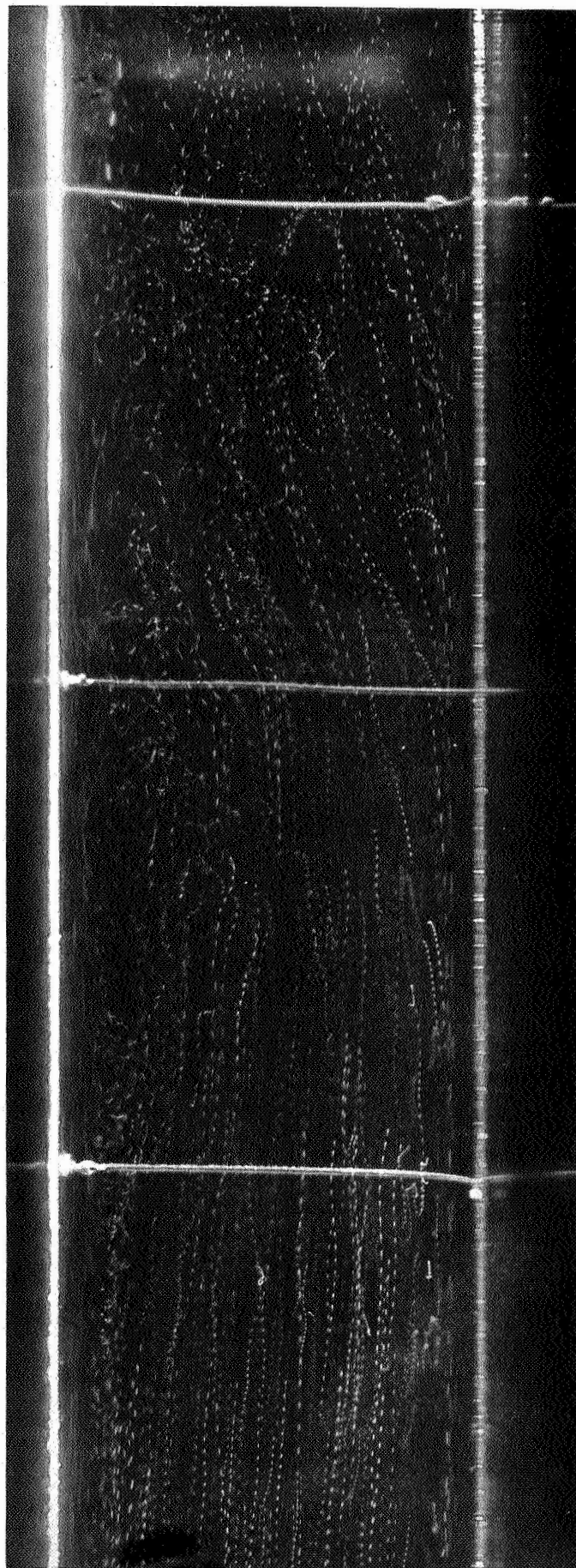


Figure 13. Flow Patterns - View Interruption Method
(see Appendix)

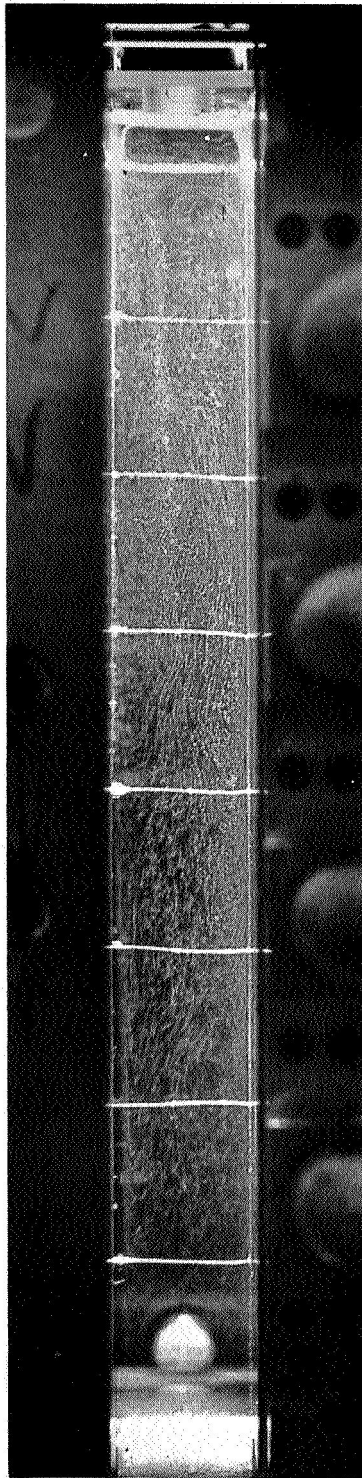


Figure 14. Flow Patterns - Entire Cell
(see Appendix)

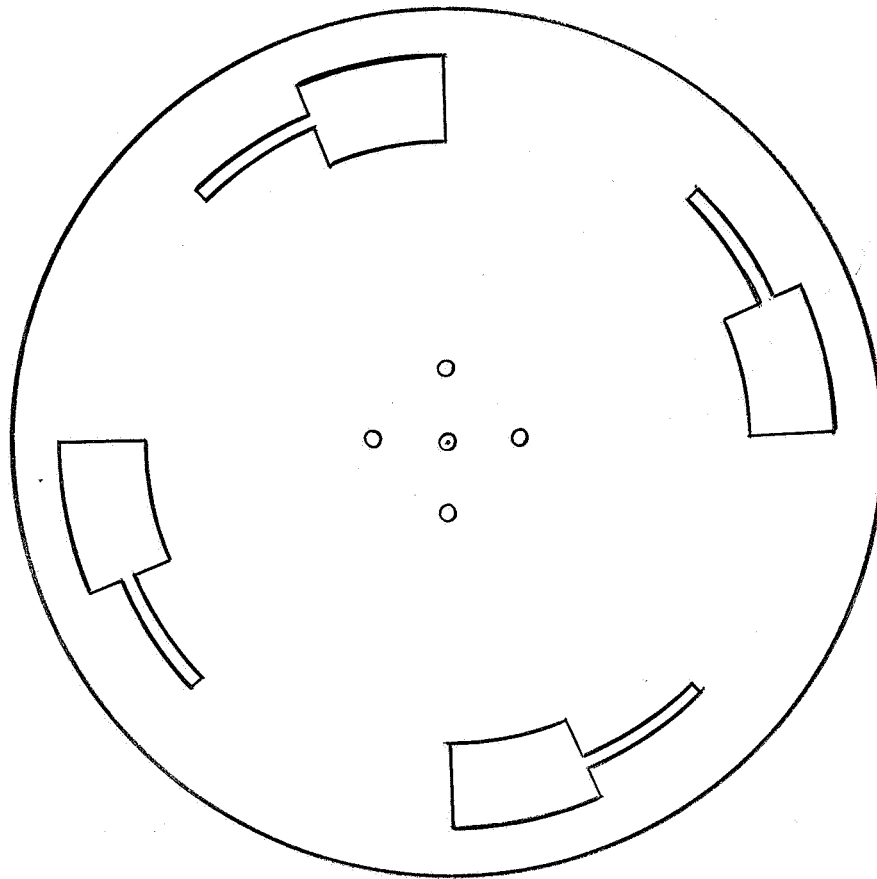


Figure 15. Flow Visualization View
Interruption Wheel.

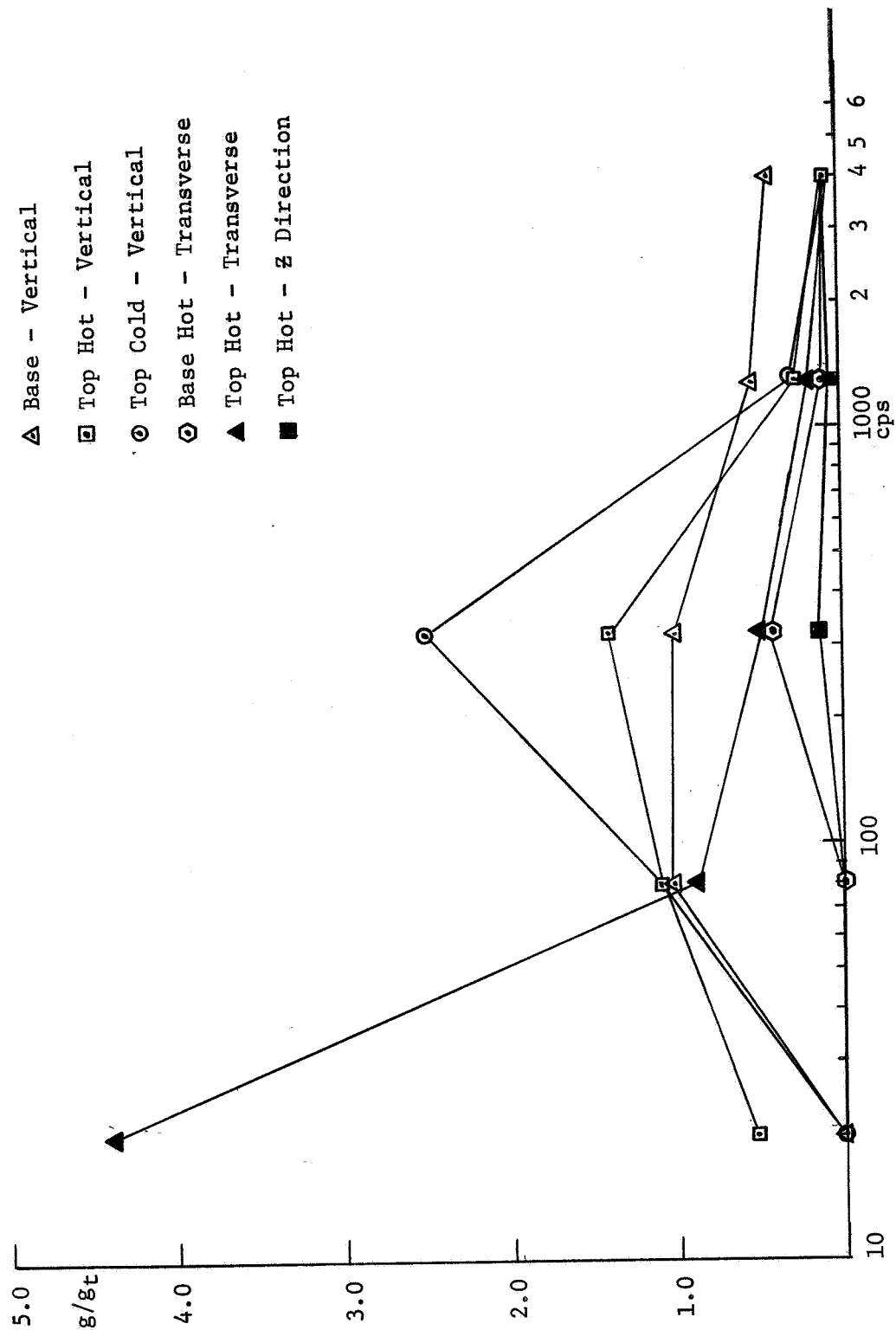


Figure 16. Acceleration Levels at Various Points on the Enclosure Relative to Table Acceleration (g_t).

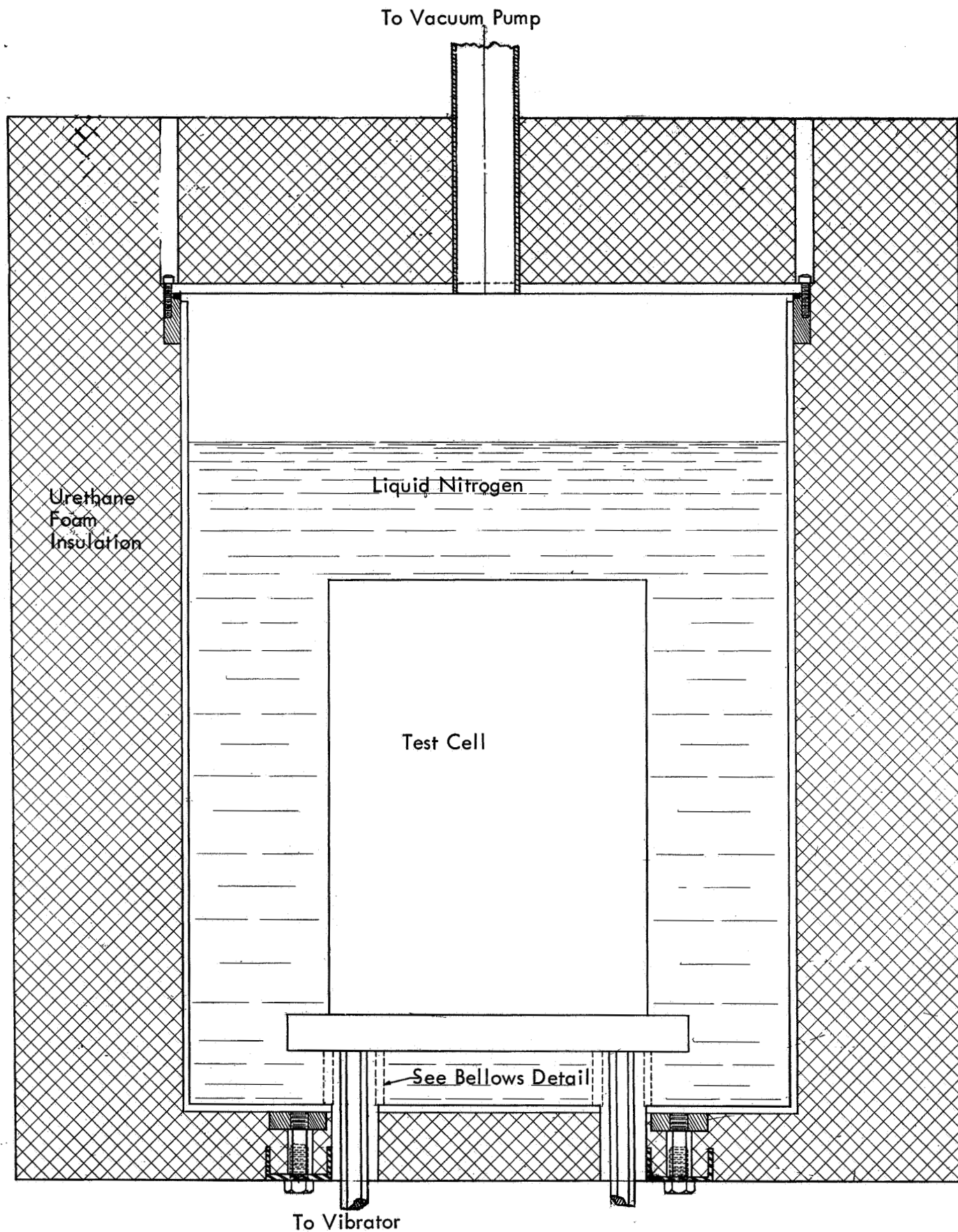


Figure 17. Liquid Nitrogen Test System

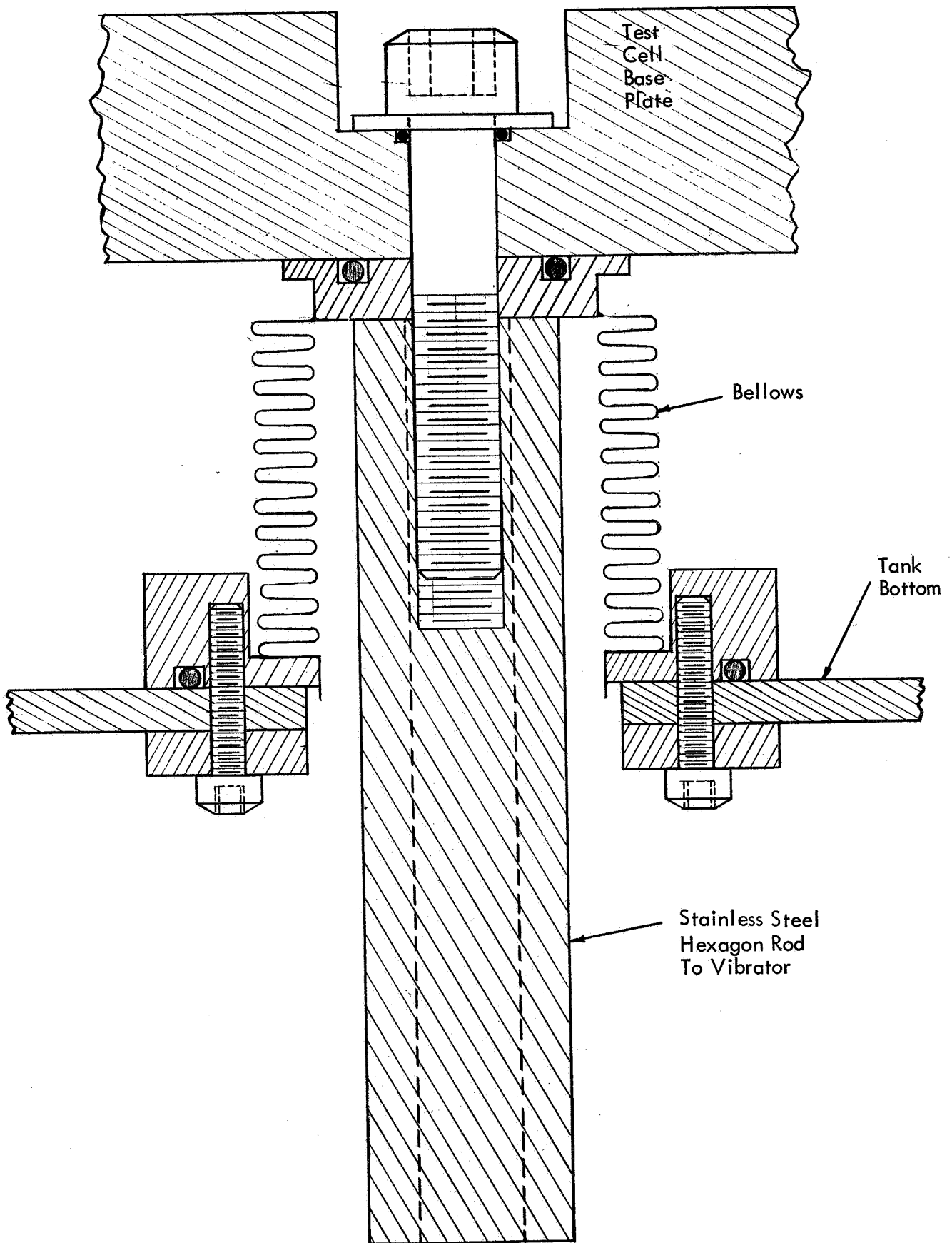


Figure 18. Bellows Mounting Detail

APPENDIX I

Discussion of Representative Flow Visualization Photographs

Figure 12 was made during vibration @ 1000 cycles per second and 25 g. $\Delta T = 37^{\circ} \text{ F}$. The photograph is a two second time exposure which allowed the moving particles to cause white streaks along their path lines thereby revealing the flow patterns. A bubble coalescence area is apparent in the upper right corner and its effect on the flow is noted.

Figure 13 was made under a no vibration condition. The separate "dots" were produced by rotating a slotted wheel placed between the camera and the test cell. This produced a series of dots which follow the path of the moving particles. Particles moving in the relatively high velocity boundary area immediately adjacent to the hot and cold plates appear as blurred streaks due to their high velocity relative to particles outside these areas. Particles may be observed as they enter the cold plate boundary region in which case the "dots" become spaced farther and farther from one another and also become blurred as the particles gain speed upon entering the high velocity region. The wheel rotation produced "dots" which in this picture are "1.122 seconds" apart.

Figure 14 is a view of the entire cell made with a ΔT of 37° F . and no vibration. Flow lines may be observed where there is an appreciable fluid velocity except in the high velocity boundary areas where again the fast moving particles yielded blurred images.